Exergy Analysis of a Combined Power and Refrigeration Thermodynamic Cycle Driven by a Solar Heat...

Article *in* Journal of Solar Energy Engineering · February 2003

DOI: 10.1115/1.1530628

2 authors:

Afif Hasan
Birzeit University

D. Yogi Goswami
University of South Florida

Afif Akel Hasan
Mechanical Engineering Department,
Birzeit University, P.O. Box 14, Birzeit,
Palestinian Authority, via Israel
e-mail: ahasan@birzeit.edu

D. Y. Goswami
Solar Energy and Energy Conversion Laboratory,
Department of Mechanical
and Aerospace Engineering,
P.O. Box 116300,
University of Florida,
Gainesville, FL 32611-6300
e-mail: solar@cimar.me.ufl.edu

Exergy Analysis of a Combined Power and Refrigeration Thermodynamic Cycle Driven by a Solar Heat Source

Exergy thermodynamics is employed to analyze a binary ammonia water mixture thermodynamic cycle that produces both power and refrigeration. The analysis includes exergy destruction for each component in the cycle as well as the first law and exergy efficiencies of the cycle. The optimum operating conditions are established by maximizing the cycle exergy efficiency for the case of a solar heat source. Performance of the cycle over a range of heat source temperatures of 320–460°K was investigated. It is found that increasing the heat source temperature does not necessarily produce higher exergy efficiency, as is the case for first law efficiency. The largest exergy destruction occurs in the absorber, while little exergy destruction takes place in the boiler.
[DOI: 10.1115/1.1530628]

1 Introduction

Binary mixture thermodynamic cycles are receiving more attention from researchers in recent years. Binary mixtures boil over a range of temperatures; as boiling progresses the temperature of the mixture increases due to the change in its composition. The change in boiling temperature leads to a good match with a sensible heat source [1–3]. The increased effectiveness in the heat transfer during the heat addition process reduces the cycle irreversibilities and improves the cycle performance.

A novel cycle that employs ammonia water binary mixture as a working fluid was proposed by Goswami [4]. As a binary mixture cycle, it has a good match between the heating fluid and the working fluid during the heat addition process. In addition, the Goswami cycle can produce both work and refrigeration, and it can utilize flat plate solar collectors with a potential reduction in the capital costs of solar thermal power by as much as 50% and applications in buildings that require power and air conditioning [4]. A schematic of the cycle is shown in Fig. 1, in which an ammonia water vapor mixture with over 99% ammonia mass fraction expands in the turbine to a temperature below the ambient temperature. An absorption process replaces the conventional heat rejection and condensation process in this cycle.

A simulation program was developed by Xu [5] for the combined power and refrigeration cycle, the program uses material and energy balances as well as the thermodynamic properties of the binary ammonia water mixture. The simulation program computes the state conditions at different locations of the cycle and the energy transfer for each component in the cycle, including work and heat transfer. Parametric study of the cycle was carried out and a range of operating conditions was suggested for the combined power and refrigeration cycle [4].

Optimization of the cycle was investigated and some optimum operating conditions were examined by Lu [6].

The combined power and refrigeration cycle can utilize different heat sources including low temperature waste heat, solar energy and geothermal energy.

In this paper, the cycle is analyzed using exergy thermodynamics. First law efficiency, exergy efficiency, and exergy destruction in the cycle are examined over a range of heat source temperatures that correspond to solar heat sources.

2 Exergy

Exergy analysis is used as a tool to enhance the understanding of thermodynamic processes and improve their performance. Exergy analysis reveals the irreversibilities in the cycle and shows the possibilities where improvements in efficiency could be made [1,7].

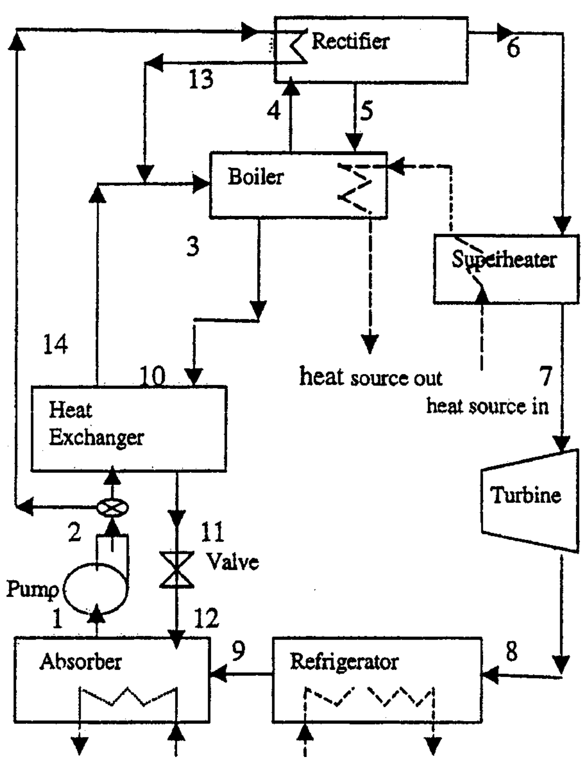

Fig. 1 Schematic of the combined power and refrigeration cycle

Contributed by the Solar Energy Division of the American Society of Mechanical Engineers for publication in the ASME JOURNAL OF SOLAR ENERGY ENGINEERING. Manuscript received by the ASME Solar Energy Division, July 2001; final revision, May 2002. Associate Editor: V. Mei.

Exergy is defined as the maximum amount of reversible work a substance can do during the process of reaching equilibrium with its surroundings [8]. If surrounding temperature T_o is taken as a reference temperature, then exergy per unit mass of a stream, ε, is given as,

$$\varepsilon=(h-h_o)-T_o(s-s_o) \tag{1}$$

where h is enthalpy, s is entropy, and the subscript o refers to reference state.

For a mixture, the exergy is given in terms of exergy of pure components evaluated at component partial pressure and mixture temperature. Szargut [8] suggested that for a binary mixture, exergy could be given in terms of enthalpy, entropy and composition of mixture as follows,

$$\varepsilon=(h-T_o s)+\alpha+\beta x \tag{2}$$

where x is the mass fraction of one component in the mixture, and α and β are two constants whose values are set arbitrarily such that exergy in the cycle is always positive. Actually the constants α and β are functions only of pure components at the reference state and their values do not change in the cycle. It can be shown using material and exergy balances that in calculating the exergy destruction in the cycle for any control volume, the constants α and β vanish and, therefore, have no effect on the value of exergy destruction in the cycle. In our calculation, α is set as 50, β is set as 250, the reference temperature T_o is 290°K, and the reference pressure is 0.1013 MPa.

Ammonia water mixture properties are calculated based on the method developed by Xu and Goswami [9].

3 Exergy Efficiency

Exergy efficiency is defined as the ratio of exergy output, E_{out}, to the exergy input. When solar thermal energy is used as a heat source the heating fluid is returned to a storage tank or to the collectors and hence its remaining exergy is not lost. Thus the exergy input is taken here as the change in exergy of the heating fluid, ΔE_{hs} as shown in Eq. (3). If the heating fluid exhausts to the environment such as in the case of a gas turbine or a geothermal resource, its exergy is lost, so the efficiency is based on the initial exergy of the heating fluid, E_{hs-in}, as given in Eq. (4).

$$\eta_{ex}=\frac{\Sigma E_{out}}{\Sigma \Delta E_{hs}} \tag{3}$$

$$\eta_{ex}=\frac{\Sigma E_{out}}{\Sigma E_{hs-in}} \tag{4}$$

In this combined power and refrigeration cycle, there are two useful outputs: power and refrigeration. Exergy of power is just the net power of the cycle W_{net}. However, the exergy E_{Q_c} of a refrigeration load Q_c is given by Zsargut [8] as,

$$E_{QC}=\frac{Q_C}{COP_C} \tag{5}$$

where COP_C is the coefficient of performance for a Carnot refrigeration cycle and is given as,

$$COP_C=\frac{T_C}{(T_O-T_C)} \tag{6}$$

where T_c is the cold reservoir temperature and T_o is the ambient temperature.

Therefore, the exergy efficiency, η_{ex}, of the combined power and refrigeration cycle may be given as,

$$\eta_{ex}=\frac{(W_{net}+Q_C/COP_C)}{\Delta \mathrm{E}_{hs}} \tag{7}$$

4 Exergy Destruction and Irreversibilities

Exergy destruction is equal to the irreversibilities as given by Guoy-Stodola equation [10]. Exergy destruction E_D is calculated by rearranging the exergy balance equation for a control volume at steady state in the following form [11,12],

$$E_D=\sum m_1\varepsilon_1-\sum m_e\varepsilon_e-W_{cv}+\sum (1-T_o/T)Q \tag{8}$$

where W_{cv} is the work of control volume, m is the mass flow rate, E_D is exergy destruction within the control volume, Q is heat transfer with surroundings or other fluids, and subscripts i and e are used for inlet and exit, respectively. Average temperature is used whenever temperature is not constant.

Irreversibility is calculated from entropy generation and ambient temperature as,

$$I=T_o S_{gen} \tag{9}$$

where I is irreversibility, and S_{gen} is the entropy generation.

5 Reversible Combined Power and Refrigeration Cycle

Figure 2 shows a simple thermodynamic representation of the combined cycle. At steady state, an energy balance for the cycle is given as,

$$Q_h+Q_c=Q_o+W_{net} \tag{10}$$

where Q_h is the heat addition from the heat source at average temperature T_h, Q_c is the refrigeration at average temperature T_c, Q_o is the heat rejection to the ambient heat sink at T_o, and W_{net} is the net power output of the cycle.

The second law for a reversible cycle, where entropy generation is zero, is given as,

$$Q_h/T_h+Q_c/T_c-Q_o/T_o=0 \tag{11}$$

by substituting Q_o from Eq. (10) and rearranging, the following equation is obtained:

$$Q_h\eta_c-Q_c/COP_c-W_{net}=0 \tag{12}$$

where the Carnot efficiency η_c is given as,

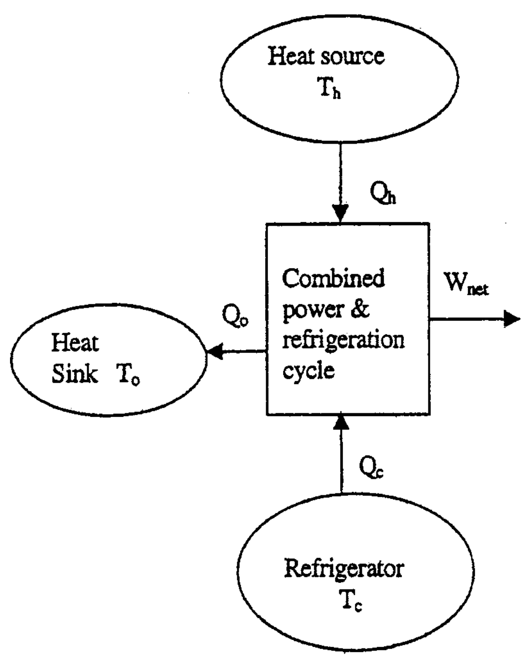

Fig. 2 Thermodynamic representation of the combined power and refrigeration cycle

Table 1 Optimized operating conditions for the combined cycle, heat source at 350°K

State point	T (K)	P MPa	Enthalpy (kJ/kg)	Entropy (kJ/kg.K)	Exergy (kJ/kg)	Concentration (kg. ammonia/kg solution)	Flow ratio mi/m1
1	295.0	0.52	−113.1	0.190	44.7	0.652	1.000
2	295.1	1.71	−111.7	0.190	46.3	0.652	1.000
3	335.1	1.71	74.2	0.780	60.9	0.652	1.000
4	344.8	1.71	1387.4	4.425	402.3	0.992	0.161
5	330.6	1.71	93.9	0.767	105.8	0.738	0.003
6	330.6	1.71	1339.8	4.283	397.0	0.997	0.157
7	338.2	1.71	1362.8	4.351	400.3	0.997	0.157
8	280.0	1.71	1207.2	4.351	244.7	0.997	0.157
9	285.0	0.52	1265.3	4.556	243.1	0.997	0.157
10	344.8	1.71	99.1	0.891	37.8	0.588	0.843
11	300.1	1.71	107.7	0.249	17.1	0.588	0.843
12	300.3	0.52	−107.7	0.254	15.7	0.588	0.843
13	325.6	1.71	29.3	0.645	55.4	0.653	0.082
14	335.9	1.71	78.2	0.793	61.4	0.653	0.918

$$\eta_c = \frac{(T_h - T_o)}{T_h} \tag{13}$$

and the COP_C for the refrigeration cycle operating between T_o and T_c is given by Eq. (6).

$Q_h \eta_c$ is the exergy of the heat source, which represents the upper limit on the output exergy from the combined cycle.

For the case of all refrigeration, and no net power, Eq. (12) simplifies to Eq. (14) which is the Coefficient of Performance of the reversible absorption refrigeration cycle, COP_R.

$$\frac{Q_c}{Q_h} = \frac{T_c(T_h - T_o)}{T_h(T_o - T_c)} = COP_R \tag{14}$$

Equation (12) gives the exergy balance for a reversible cycle, while the exergy balance for an irreversible cycle includes the exergy destruction term E_D, as shown below,

$$Q_h \eta_c - Q_c / COP_c - W_{net} = E_D \tag{15}$$

The exergy for refrigeration as given in the exergy balance Eq. (12) is the same as given earlier in Eq. (5).

6 Maximizing the Exergy Efficiency

The operating conditions of the combined cycle are found by maximizing the exergy efficiency of the cycle. Exergy efficiency is a measure of the closeness of the cycle to the reversible one.

The optimization program and procedure are described in detail by Lu [6]. The program uses the Generalized Reduced Gradient algorithm developed by Lasdon et al. [13]. The optimization starts with an initial guess of the variables to be optimized and iterates until a maximum is obtained for the specified objective function subject to certain specified constraints.

7 Results and Discussion

7.1 Typical Operating Conditions. Table 1 shows typical optimum operating conditions for the combined cycle. An inlet heating source temperature of 350°K, an absorber temperature 295°K and an ambient temperature of 290°K are used in the optimization. The state points in the first column of the table correspond to the locations given in Fig. 1 of the cycle schematic.

The ammonia fraction coming out of the boiler is very high 99.2%, therefore, little rectification is needed. At operating conditions with higher pressures, the ammonia fraction would be lower in the boiler and condensation of some water vapor would be necessary in the rectifier.

The low temperature in the cycle, 280°K, exists at the exit of the turbine, this temperature is lower than the ambient temperature, and thus refrigeration can be produced through heat transfer to the working fluid in the cycle. The pressure ratio across the turbine is low at 3.3, thus small amount of power is produced from the cycle at the above operating conditions. Only 16% of the basic solution flows through the turbine and the refrigerator producing power and refrigeration, while the rest of the solution returns to the absorber. Exergy in the cycle is highest at the inlet of the turbine, where it has the highest potential of doing work. Exergy is lowest where the weak ammonia solution returns to the absorber. At the entrance of the refrigerator the working fluid still has a considerable amount of exergy, though the temperature is below the ambient. The exergy values in Table 1 are relative ones and, absolute exergy values can be calculated by adding the chemical exergy at the dead state to the above given physical exergy [8,14].

Table 2 Energy transfer in the cycle for operating conditions in Table 1

Part of Cycle	Energy Transfer (kW)
Boiler heat input	231.8
Super heater input	3.6
Total heat addition to cycle	235.4
Solution heat exchange	174.2
Rectifier heat rejection	11.6
Absorber heat rejection	221.6
Refrigeration output	9.1
Turbine power output	24.5
Pump power input	1.5
Cycle net power	23.0

7.2 Energy Analysis. Table 2 shows the energy transfer for different parts in the cycle for the conditions of Table 1, and assuming 1 kg/s as the flow rate of basic solution. In this simulation, it is assumed that the turbine and the pump are both isentropic, throttling process in the valve is a constant enthalpy one, and pressure losses are negligible in the cycle.

The first law efficiency for the combined cycle is calculated as given in Eq. (16),

$$\eta_1 = \frac{(W_{net} + Q_c)}{Q_h} \tag{16}$$

The first law efficiency includes both useful outputs: the power W_{net} and the refrigeration Q_c. Heat input includes the heat added to the cycle in both the boiler and the superheater. The efficiency of the optimized cycle at the conditions shown in Table 1 is 13.6%. A Carnot heat engine operating between 350°K and 290°K would have a thermal efficiency of 17.2%. The combined power and refrigeration cycle has an efficiency, which is 79.1% of the Carnot efficiency at the optimum operating conditions in Table 1. A Lorenz cycle, which is a reversible cycle that accounts for a

Table 3 Exergy destruction and irreversibilities, heat source temperature 350°K

Part of Cycle	Irreversibilities (kW)	Exergy Destruction (kW)	Percent of Total
Boiler	1.7	1.7	11.8
Superheater	0.1	0.1	0.7
Solution heat exchanger	3.4	3.4	23.6
Rectifier	1.0	1.0	6.9
Absorber	6.8	6.8	47.2
Refrigerator	0.1	0.1	0.7
Turbine	0.0	0.0	0.0
Pump	0.0	0.0	0.0
Mixing at boiler inlet	0.0	0.1	0.7
Pressure valve	1.2	1.2	8.3
Total cycle	14.4	14.4	100

sensible heat source as opposed to a constant temperature heat source of the Carnot cycle [5,15] is more appropriate for comparison with this cycle. The efficiency of a Lorenz cycle operating between the same conditions would be 15.9%.

7.3 Exergy Destruction. Table 3 shows the irreversibilities and exergy destruction in the cycle. Exergy destruction is calculated using Eq. (8), and irreversibilities by using Eq. (9). As expected by the Guoy-Stodola equation, exergy destruction and irreversibilities are the same. As explained earlier, the turbine and the pump are assumed isentropic. Irreversibilities in the refrigerator are close to zero since the heat transfer in the refrigerator is relatively small and occurs at temperatures close to the ambient. The absorber has the highest irreversibilities at 47.2% of the total cycle irreversibilities, next is the solution heat exchanger at 23.6%, followed by the boiler at 11.8% and then the pressure-reducing valve. The absorber has the highest irreversibilities since it involves two highly irreversible processes of condensation and mixing of ammonia and water components. The solution heat exchanger involves the process of heat exchange between the two streams of strong and weak ammonia solutions with a large temperature difference. The boiler involves the boiling process, which is irreversible.

Exergy efficiency for the cycle, as defined in Eq. (7), and at the operating conditions of Table 1, is 61.8%. Hence 39.2% of the heat source exergy change is being lost in the cycle, these losses are in the form of exergy destruction, and exergy losses from the absorber during the heat rejection process to the environment.

The total exergy destruction is also calculated using the exergy balance Eq. (15), which gives a total exergy destruction of 14.4, the same as in Table 3. Average temperatures are used in calculating the Carnot efficiency and COP in Eq. (15).

7.4 Effect of Heat Source Temperature. The optimum performance of the combined cycle was examined over a heat source inlet temperature range of 320–460°K. This low and medium temperature range can be obtained from flat plate collectors or medium temperature concentrators. Figure 3 shows the effect of heat source temperature on the performance of the cycle, including net power and refrigeration capacity as a fraction of the heat addition, first law efficiency and exergy efficiency.

The refrigeration, as a fraction of the heat addition Q_c/Q_h, changes little as the heat source temperature increases. As temperature of the heat source approaches the ambient temperature, refrigeration approaches zero. The highest refrigeration fraction is around a source temperature of 390°K. The refrigeration fraction decreases above this source temperature and becomes zero around 480°K.

The net power, as a fraction of heat addition W_{net}/Q_h, increases as the heat source temperature increases. Since the turbine output power is related mainly to the pressure ratio across the turbine, net cycle power curve can be explained in relation to the pressure ratio in Fig. 4, which shows a continuous increase with the heat source temperature.

The first law efficiency curve, which is the sum of the refrigeration and power curves, shows a corresponding behavior to the power curve up to a maximum value of 23.6% at 440°K. After the maximum point, the efficiency starts decreasing slowly in a similar behavior to the refrigeration curve.

The exergy efficiency shows a maximum value of 65.2% at 380°K. The sharp increase in the exergy efficiency between 320 and 380°K is due to the increase of both outputs, the net power and refrigeration, as shown in the same figure. Refrigeration

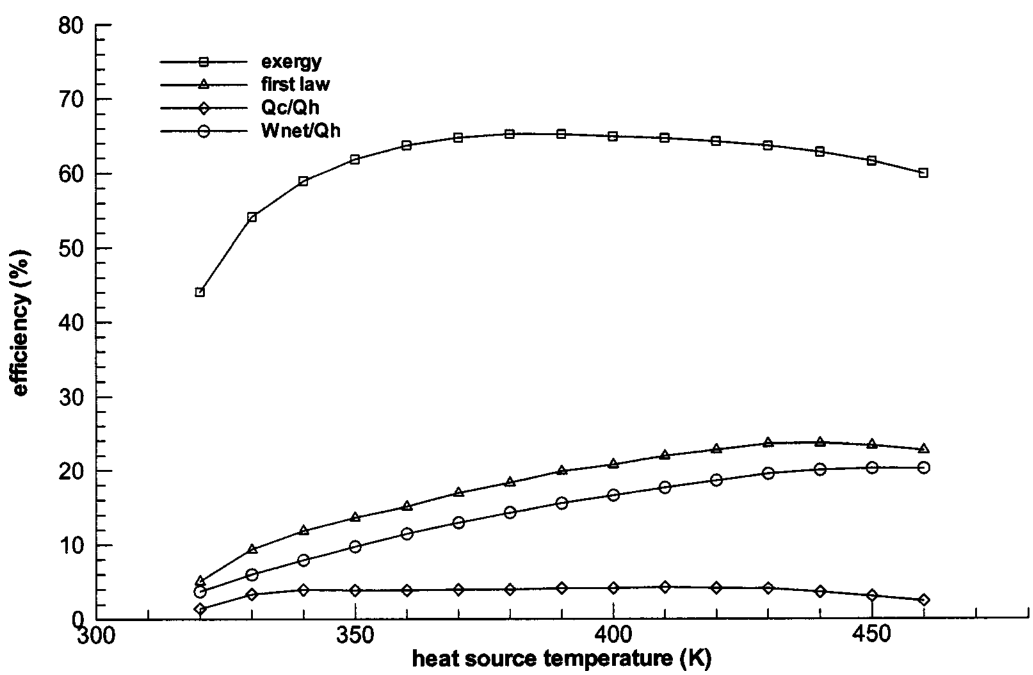

Fig. 3 Efficiency versus heat source temperature

decreases above 400°K while the net power continues to increase slowly, the net result being that the exergy curve shows a maximum.

Figure 5 shows the refrigeration to net power ratio versus the heat source temperature. The maximum refrigeration to net power ratio occurs at 330°K. Increasing the heat source temperature above 330°K would favor the production of net power rather than refrigeration.

Figure 6 shows normalized exergy destruction in the cycle as a function of the heat source temperature. Total exergy destruction in the cycle increases with an increase in the heat source temperature. It can be seen in Fig. 6 that exergy destruction in both absorber, and heat exchanger change little as the source temperature increases. Superheater has almost zero exergy destruction because of its small heat load. The boiler exergy destruction is much lower than the absorber. Exergy destruction in the rectifier increases as the heating load in the rectifier increases as depicted in Fig. 7, and becomes the largest above 420°K. Therefore, to improve the design of the cycle, the rectifier may be eliminated above a heat source temperature of 420°K, especially if low temperature (<273°K) refrigeration is not required.

From an exergy efficiency point of view, if the heat source is between 320 and 460°K, then the best operating heat source temperature is around 380°K, since it gives the maximum exergy efficiency. A solar heat source using a flat plate collector at 360°K (87°C) gives an exergy efficiency of 63.7%, with refrigeration as 3.7% of the heat addition and net power as 11.5% of the heat addition to the combined cycle.

8 Conclusions

The combined power and refrigeration cycle, operating under optimum conditions, can produce different fractions of power and refrigeration depending on its heat source temperature.

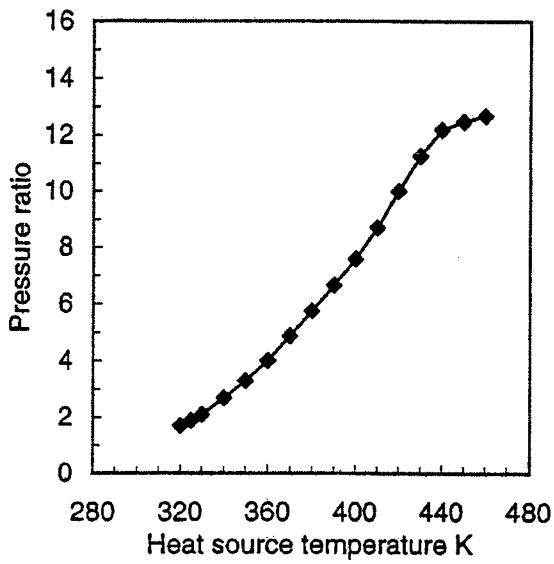

Fig. 4 Pressure ratio versus heat source temperature

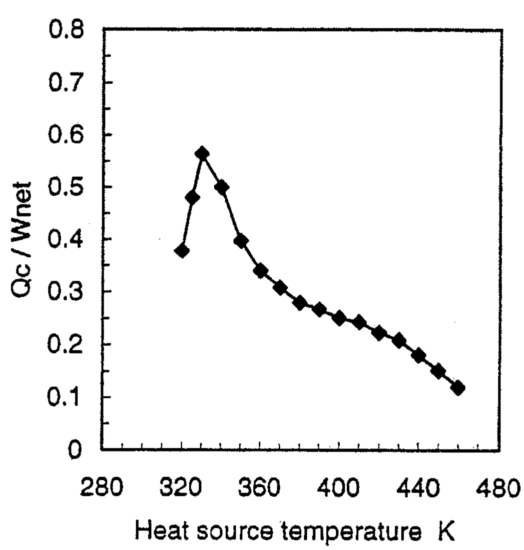

Fig. 5 Refrigeration to net power ratio versus heat source temperature

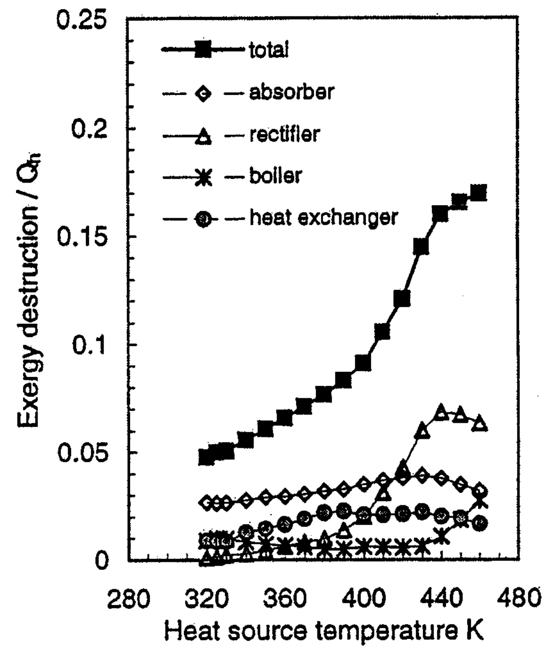

Fig. 6 Normalized exergy destruction versus heat source temperature

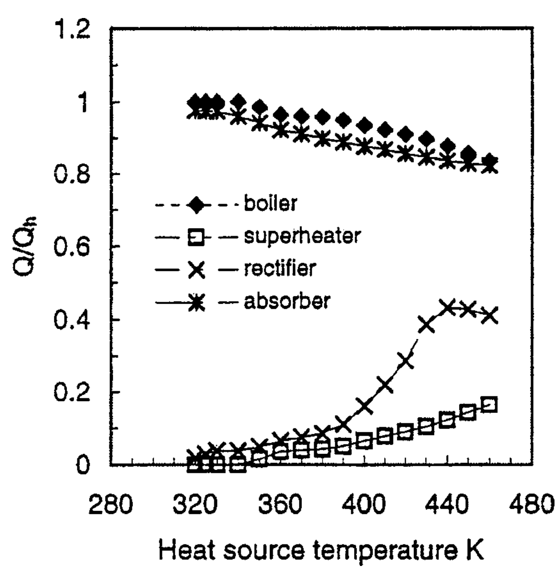

Fig. 7 Normalized heat transfer versus heat source temperature

Exergy analysis can be used to improve the cycle performance. Total exergy destruction in the combined power and refrigeration cycle increases as the heat source temperature increases. The absorber has the highest exergy destruction for a heat source temperature of 320 to 400°K, while above 400°K the rectifier would have the highest contribution to the exergy destruction in the cycle. The boiler has moderate contribution to the cycle exergy destruction. This leads us to a conclusion that it may be better to eliminate the rectifier for source temperatures above 400°K, especially if low temperature refrigeration below 273°K is not required. The results also lead us to a study of a better absorber.

The exergy efficiency has a maximum point over the investigated range of 320–460°K heat source temperatures. Increasing the heat source inlet temperature does not necessarily lead to higher exergy efficiency as it is the case for Carnot thermal efficiency and the first law efficiency.

Heat from flat plate solar collectors (temperature of 90°C or less) can drive the combined power and refrigeration cycle, and produce power and refrigeration at the same time. The cycle has a good thermal efficiency reaching 25.3% at 430°K, which constitutes 78% of the Carnot engine efficiency operating between the same upper and lower boundary conditions.

Acknowledgments

One of the authors, Afif Akel Hasan, acknowledges the support of the Fulbright Research Scholarship during which this work was carried out.

Nomenclature

COP_C = coefficient of performance for a Carnot refrigeration cycle
COP_R = coefficient of performance for a reversible absorption refrigeration cycle
h = specific enthalpy, kJ/kg
I = irreversibility, kW
m = mass flow rate, kg/s
Q = rate of heat transfer, kW
s = specific entropy, kJ/kg.K
S = rate of entropy, kW/k
T = temperature, K
W = power, kW
x = ammonia mass fraction

Greek Symbols

α = constant
β = constant
ε = specific exergy, kJ/kg
E = rate of exergy, kW
Δ = change
η = efficiency

Subscripts

1 = first law of thermodynamics
abs = absorber
c = cooling
C = Carnot cycle
cv = control volume
D = destruction
e = exit
ex = exergy
gen = generation
h = heat addition
hs = heat source
i = inlet
net = net
o = reference or ambient state
Q = heat transfer
rev = reversible

References

[1] Kalina, A. I., 1984, ‘‘Combined Cycle System With Novel Bottoming Cycle,’’ ASME J. Eng. Gas Turbines Power, **106**, 737–742.
[2] Kanlina, A. I., and Leibowitz, H. M., 1987, ‘‘Applying Kalina Technology to a Bottoming Cycle for Utility Combined Cycles,’’ ASME paper 87-GT-35.
[3] Ibrahim, O. M., and Klein, S. A., 1996, ‘‘Absorption Power Cycles,’’ Energy (Oxford), **21**, 21–27.
[4] Goswami, D. Y., and Xu, F., 1999, ‘‘Analysis of a New Thermodynamic Cycle for Combined Power and Cooling Using Low and Medium Temperature Solar Collectors,’’ ASME J. Sol. Energy Eng., **121**, 91–97.
[5] Xu, F., 1997, ‘‘Analysis of a Novel Combined Thermal Power and Cooling Cycle Using Ammonia-Water Mixture as a Working Fluid,’’ Ph.D. thesis, Univ. of Florida.
[6] Lu, S., 2001, ‘‘Combined Power/Cooling Cycle,’’ Ph.D. thesis, Univ. of Florida.
[7] Mcllvried, H. G., Ramezan, M., Enick, R. M., and Venkatasubramanian, S., 1998, ‘‘Exergy and Pinch Analysis of Advanced Ammonia-Water Coal Fired Power Cycle,’’ Proc. of ASME Advanced Energy Systems, **38**, 197–203.
[8] Szargut, J., Morris, D. R., and Steward, F. R., 1988, *Exergy Analysis of Thermal, Chemical, and Metallurgical Processes*, Hemisphere Publishing Corp., New York.
[9] Xu, F., and Goswami, D. Y., 1999, ‘‘Thermodynamic Properties of Ammonia-Water Mixture for Power Cycle Applications,’’ Energy (Oxford), **24**, 525–536.
[10] Kotas, T. J., Mayhew, Y. R., and Raichura, R. C., 1995, ‘‘Nomenclature for Exergy Analysis,’’ Proc. IMechE., **209**, 275–279.
[11] Bejan, A., Tsatsaronis, G., and Moran, M., 1996, *Thermal Design and Optimization*, John Wiley and Sons Inc., New York.
[12] Moran, M. J., and Sciubba, E., 1994, ‘‘Exergy Analysis: Principles and Practice,’’ ASME J. Eng. Gas Turbines Power, **116**, 285–290.
[13] Lasdon, L. S., Waren, A. D., Jain, A., and Ratner, M., 1978, ‘‘Design and Testing of a Generalized Reduced Gradient Code for Nonlinear Programming,’’ ACM Trans. Math. Softw., **4**, 34–50.
[14] Hinderink, A. P., Kerkhof, F. P., Lie, A. B., Arons, J. De Swaan, and Van der Kooi, H. J., 1996, ‘‘Exergy Analysis With a Flowsheeting Simulator-I,’’ Chem. Eng. Sci., **51**, 4693–4700.
[15] Alefeld, G., 1989, ‘‘Second Law Analysis for an Absorption Chiller,’’ *Newsletter of the IEA Heat Pump Center*, **7**, 54–57.